

# Amplitudes and energy fluxes of simulated decay-less kink oscillations

K. Karamelas<sup>1</sup>, T. Van Doorselaere<sup>1</sup>, A. Afanasev<sup>1</sup>, D. J. Pascoe<sup>1</sup>, M. Guo<sup>2,1</sup>, P. Antolin<sup>3</sup>

<sup>1</sup>Centre for mathematical Plasma Astrophysics, Department of Mathematics, KU Leuven

<sup>2</sup>Institute of space sciences, Shandong University, Weihai 264209, China

<sup>3</sup>School of Mathematics and Statistics, University of St. Andrews

E-mail: [kostas.karamelas@kuleuven.be](mailto:kostas.karamelas@kuleuven.be)

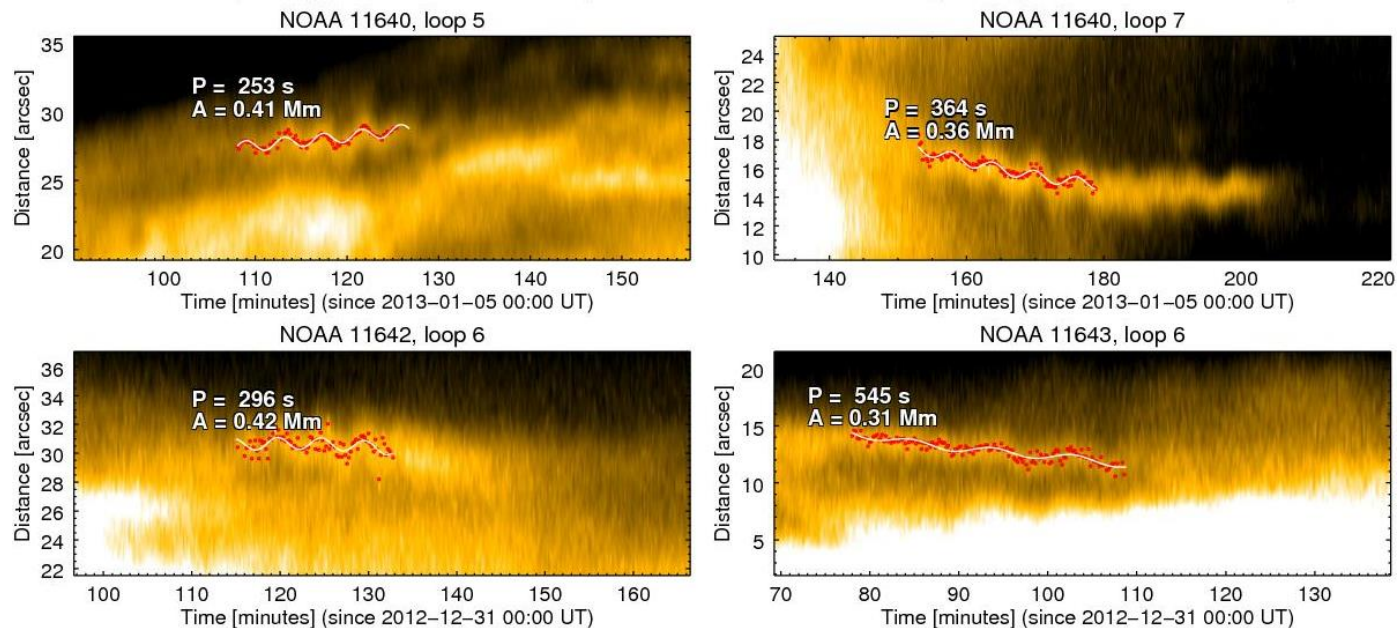


**Figure:** (Left panel) Time-distance maps of the oscillating loops. Adapted from Anfinogentov et al. (2015).

## Decayless oscillations in coronal loops

- Transverse waves of near constant amplitude  $\sim 0.1 - 0.4$  Mm (Nistico et al. 2013, Anfinogentov et al. 2015, Duckenfield et al. 2018).
- They are treated as (a) a self-oscillatory process (Nakariakov et al. 2016), (b) LOS effects from the KHI (Antolin et al. 2016), (c) driven waves (Karampelas et al. 2019a,b; Guo et al. 2018;...), or mode conversion from p modes (Riedl et al. 2019).
- Nistico et al. 2013:

*“Before and after the occurrence of a flare, the loops experience low-amplitude decayless oscillations... the periods of the kink oscillations in both cases (decaying and decayless, for the same loop) are similar ( $\sim 240$  s)... damped linear oscillator excited **by a continuous low-amplitude harmonic driver** and by an impulsive high-amplitude driver...”*

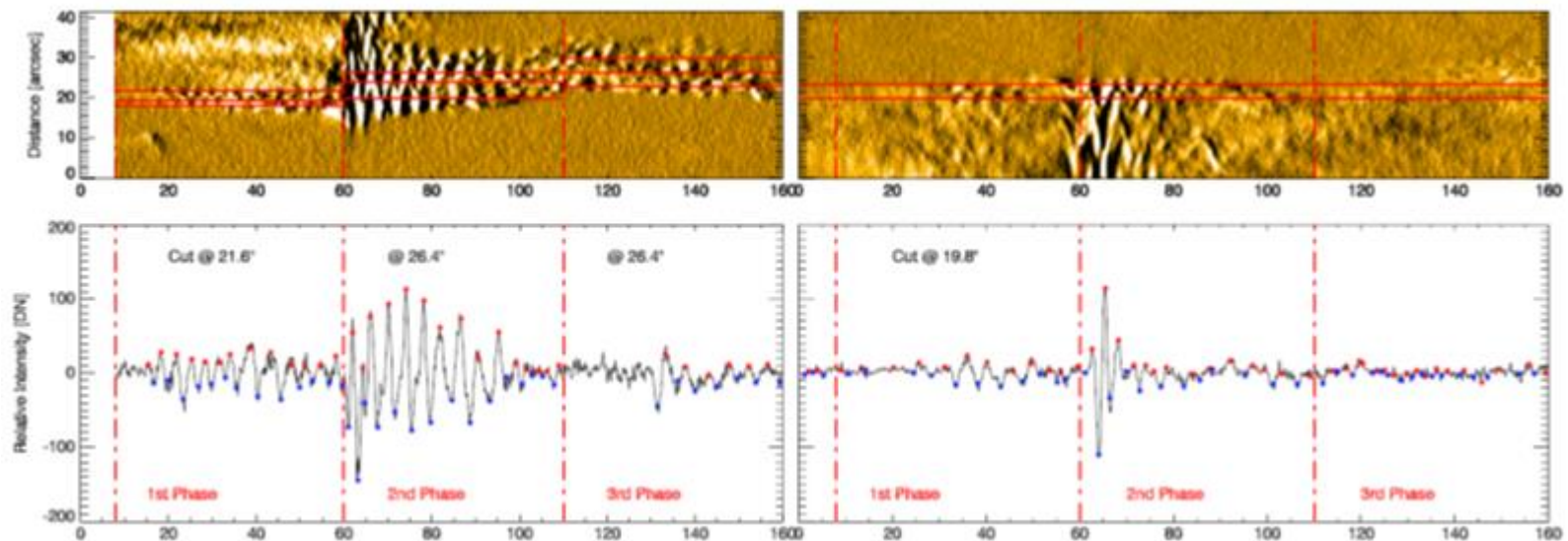


**Figure:** Time-distance maps for a moving (left panel) and steady (right panel) slit of an oscillating coronal loop. The respective zoomed parts are shown in the bottom panels. Adapted from Nistico et al. (2013).

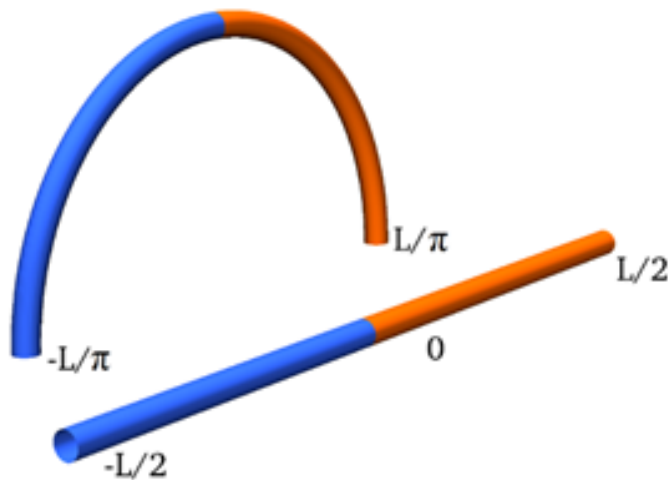


**Figure a:** Schematic representation of semi-circular loop and its corresponding straight flux tube.

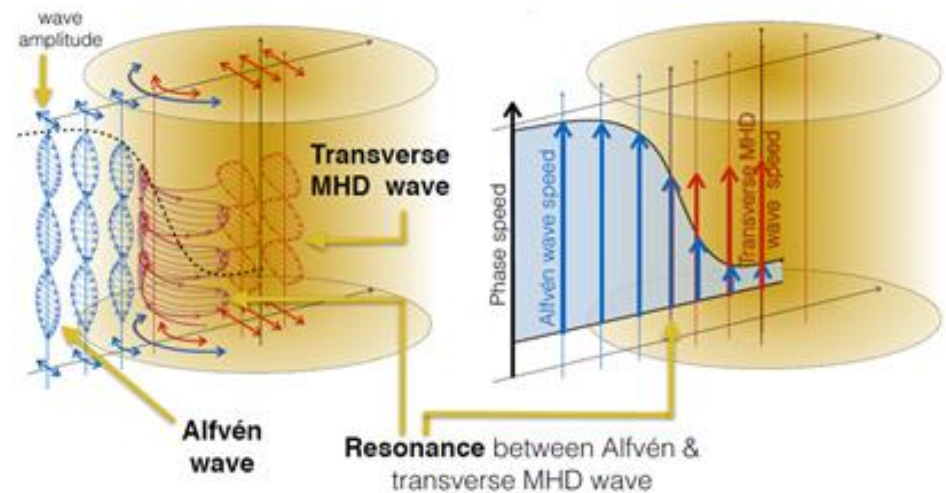


**Figure b:** Schematic representation of resonant absorption for transverse waves in a flux tube.  
Credit: Dr. Patrick Antolin, Dr. Joten Okamoto (JAXA)

## Flux tubes and standard view of wave heating in loops

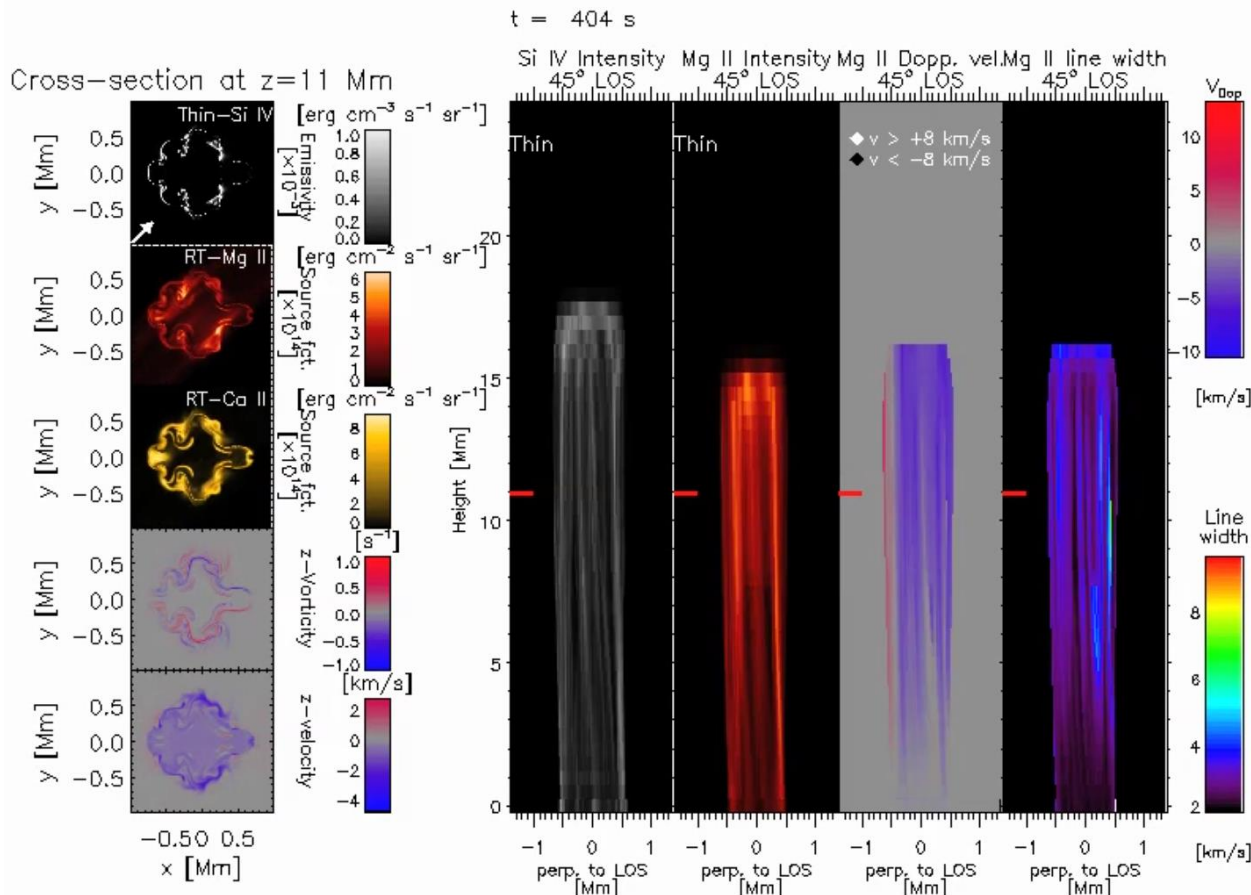
1. Flux tubes can model a variety of environments (loops, spicules and prominences)
2. Theory of wave propagation in F.T. (e.g. Zajtsev & Stepanov, 1975; Edwin & Roberts, 1983)
3. Resonant absorption / mode coupling (e.g. Goossens et al. 1992; Pascoe et al. 2010).
4. Phase mixing: (e.g. Heyvaerts & Priest, 1983; Soler & Terradas, 2015).
5. Dissipation of energy at the resonant layer.

*Transverse wave*  $\xrightarrow{\text{R.A., M.C.}}$  *azimuthal motions*  $\xrightarrow{\text{Phase mixing}}$  *small scales*  $\xrightarrow{\text{res., visc.}}$  *dissipation*

## KHI from standing transverse waves

Standing waves: Kelvin-Helmholtz unstable (Heyvaerts & Priest 1983; Poedts et al. 1997; Terradas et al 2008; Antolin et al. 2014; Zaqarashvili et al. 2015; Hillier et al. 2018, 2019; Barbulescou et al. 2019)

- 3D simulations of KHI in standing kink modes (e.g. Terradas et al. 2008; Antolin et al. 2014, 2015, 2016, 2017, 2018, 2019; Magyar et al. 2015, 2016; Howson et al. 2017a,b; Pagano et al. 2018; ...)
- 3D simulations of KHI in driven kink oscillations (e.g. Karampelas et al. 2017, 2018, 2019a,b; Guo et al. 2018, 2019; Afanasev et al. 2019)



**Movie:** KHI development in a spicule model. Movie adapted from Antolin et al. 2018.



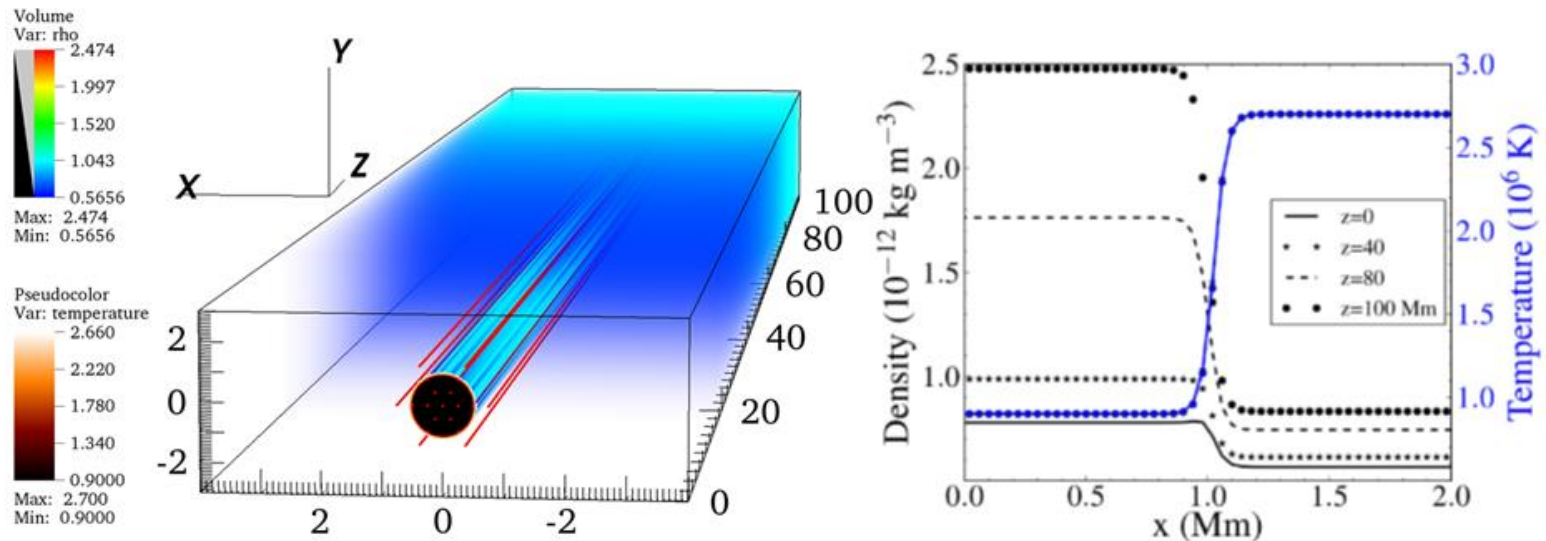


**Figure:** (Left) 3D plot of density (in  $10^{12} \text{ kg m}^{-3}$ ) for model **D2** at  $t = 0$  (left) and  $t = 15 P$  (right). Contour plots for temperature (MK) at the apex (0 Mm) and magnetic field lines (in red) are shown. (Right) density and temperature profile.

### Aims of the current study

- Reproduce the observed amplitudes of decayless oscillations in coronal loops
- Correlate the amplitudes with the input energy fluxes.

### Numerical models (from Karamelas et al. 2019b):

- 3D gravitationally stratified straight flux tube
- Simple monoperiodic footpoint driver
- $B \sim 22,8 \text{ G}$
- Models **D1**, **D2**, **D4**, **D6** and **D8**, with respective footpoint drivers of  $v_0 = 1, 2, 4, 6$  and  $8 \text{ km s}^{-1}$

## Dynamical evolution

- Driving frequency equal to the fundamental standing kink mode for a straight flux tube (Edwin & Roberts, 1983; Andries et al. 2005).
- Transverse standing waves for loops, resembling the fundamental kink mode (Karampelas et al. 2017, 2019a; Guo et al. 2018, 2019; Afanasev et al. 2019).
- Development of spatially extended **Transverse Wave-Induced Kelvin-Helmholtz (TWIKH)** rolls with the use of a continuous driver.
- Extensive mixing of plasma between the flux tube and the surrounding plasma.

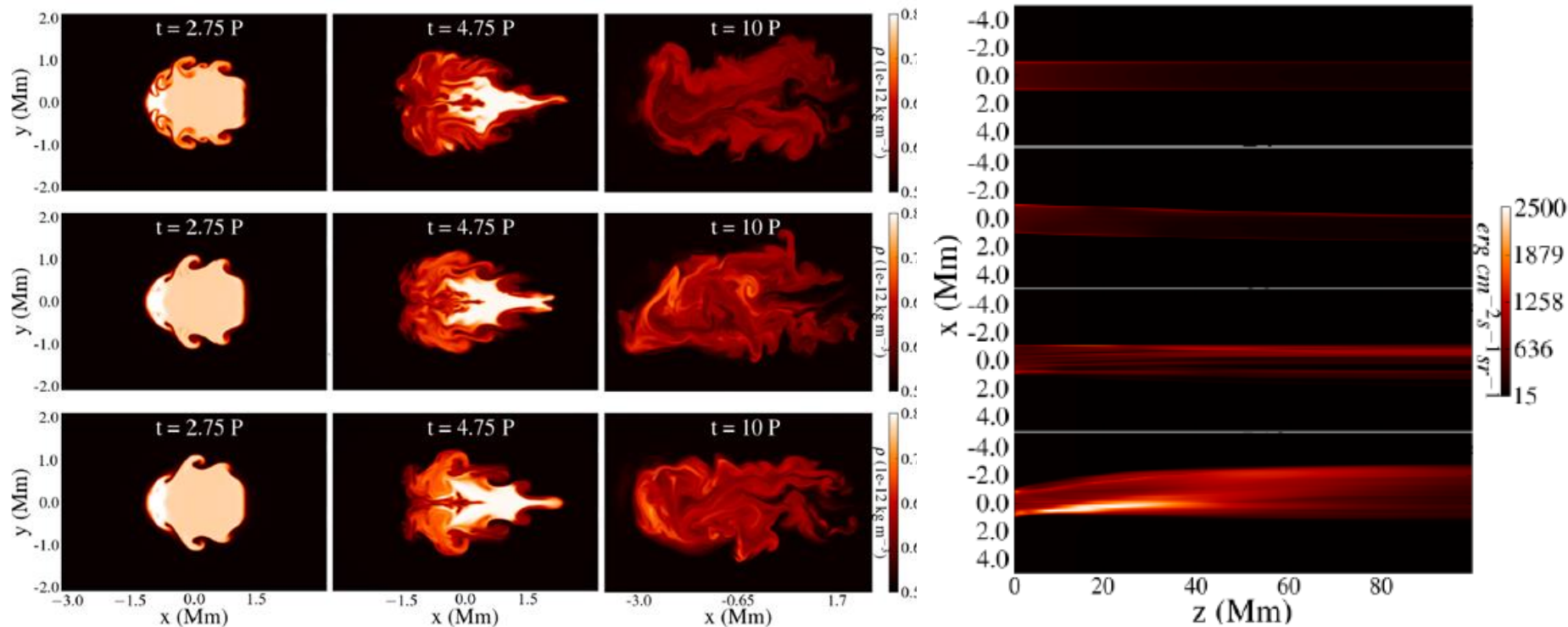


**Figure:** Loop cross-section at the apex for ideal (top), resistive (middle) and viscous (bottom) MHD. **Movie:** Emission intensity for the 195 Å. Adapted from Karampelas et al. 2019a.

## Dynamical evolution

- The development of **TWIKH** rolls leads to extensive mixing of plasma and to an apparent temperature increase inside the loop (Van Doorselaere et al. 2018).
- Very high values of viscosity ( $R_e = 10^2$ ) can suppress the KHI.
- In the case of very strong dissipation (here viscosity) the suppression of KHI leads to no mixing effects.
- No direct observation of KH instability in such systems, yet!

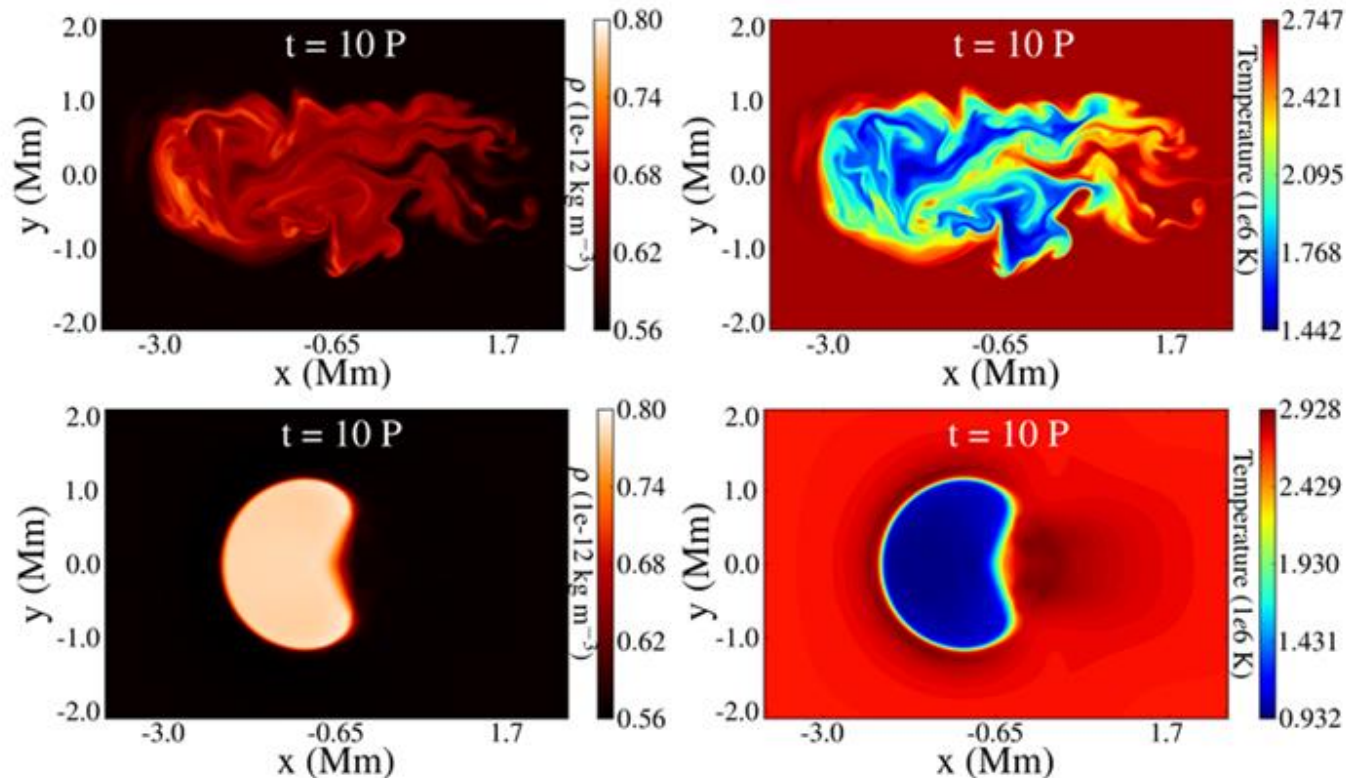


**Figure:** Loop cross-section at the apex for two different values for viscosity ( $R_e = 10^4$  for the top panel and  $R_e = 10^2$  for the bottom panel). Density (left) and temperature (right) contours are shown at the apex.

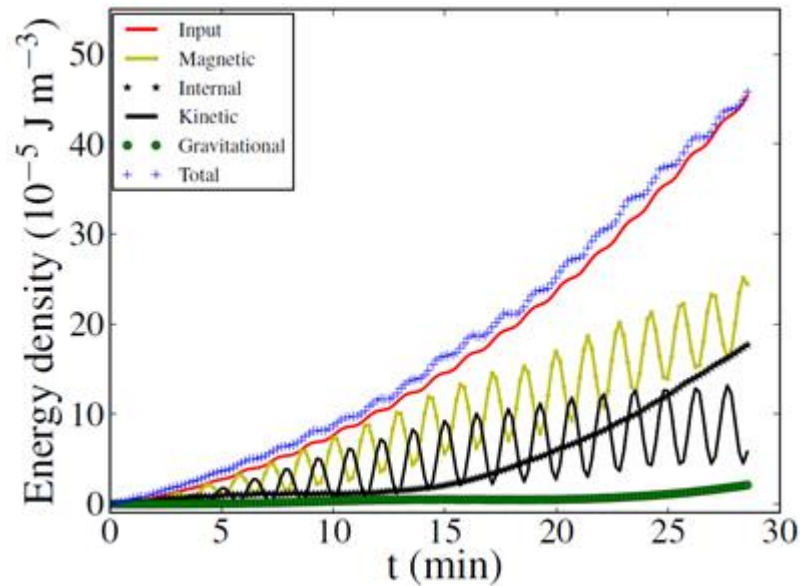


**Figure:** Input energy from the driver and average energy densities minus the fluxes from the open side boundaries.

## Energy evolution

- We calculate the energy density variation due to the Poynting flux ( $S_{tot}$ ) and the plasma flow ( $F_{tot}$ ) from the side boundaries (Belien et al. 1999; Karampelas et al. 2017, 2019a; Guo et al. 2019):

$$S_{tot} = -\frac{1}{V} \int_0^t \int_A [\eta \mathbf{J} \times \mathbf{B} - (\mathbf{v} \times \mathbf{B}) \times \mathbf{B}] \cdot d\mathbf{A}' dt',$$

$$F_{tot} = -\frac{1}{V} \int_0^t \int_A \left( \frac{\rho v^2}{2} + \rho \Phi + \frac{\gamma}{\gamma - 1} p \right) \mathbf{v} \cdot d\mathbf{A}' dt'$$



# Emission maps from simulations of decayless oscillations

Numerical models (from Karampelas et al, 2019b):

- Forward modelling with the FoMo code (Van Doorselaere et al. 2016), for different lines and angles of observations. Degradation of the synthetic data to SDO/AIA and Hinode/EIS resolution.
- We tracked the 'edge' of the loop from the synthetic data acquiring the oscillations amplitudes.
- We calculate the input energy flux for each different driver.
- We correlate the amplitudes with the input energy fluxes.

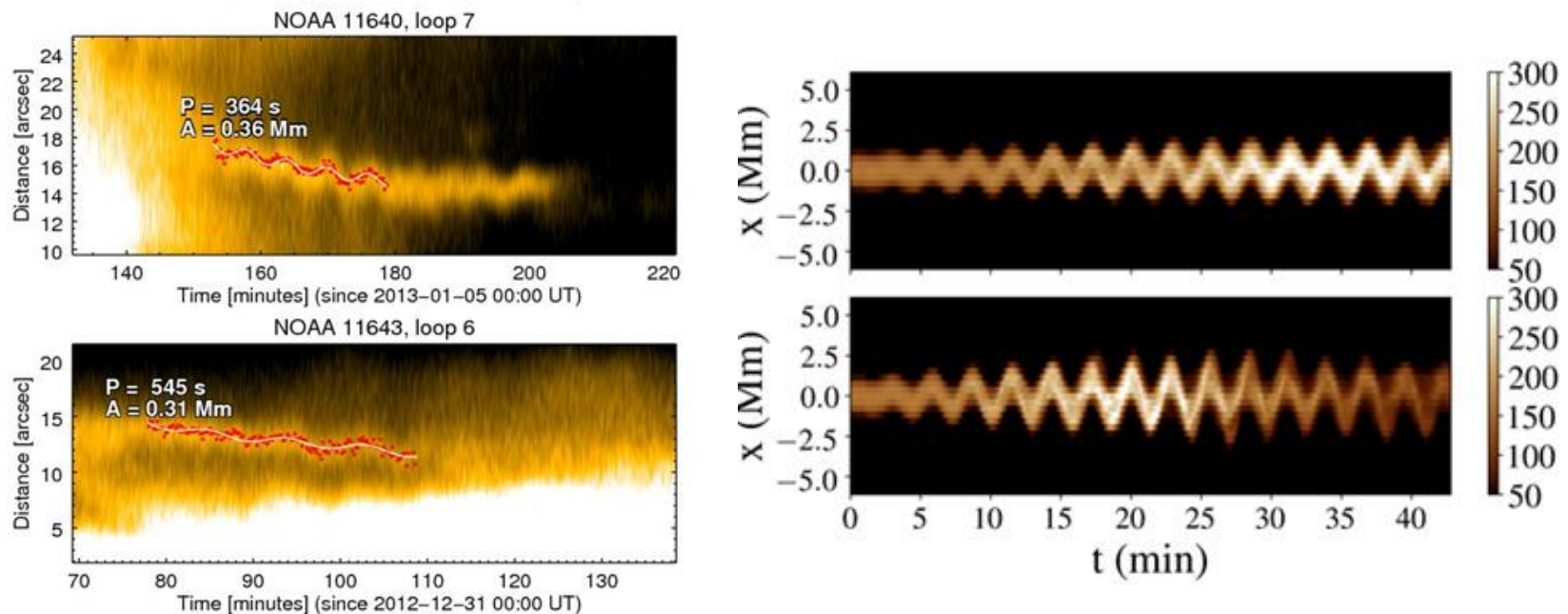


**Figure:** (Left panel) Time-distance maps of the oscillating loops. Adapted from Anfinogentov et al. (2015). (Right panel) Time distance maps of the integrated emission for models **D2** and **D4**, for the SDO/AIA 193 channel, in AIA resolution, at a  $45^\circ$  angle from the POS.

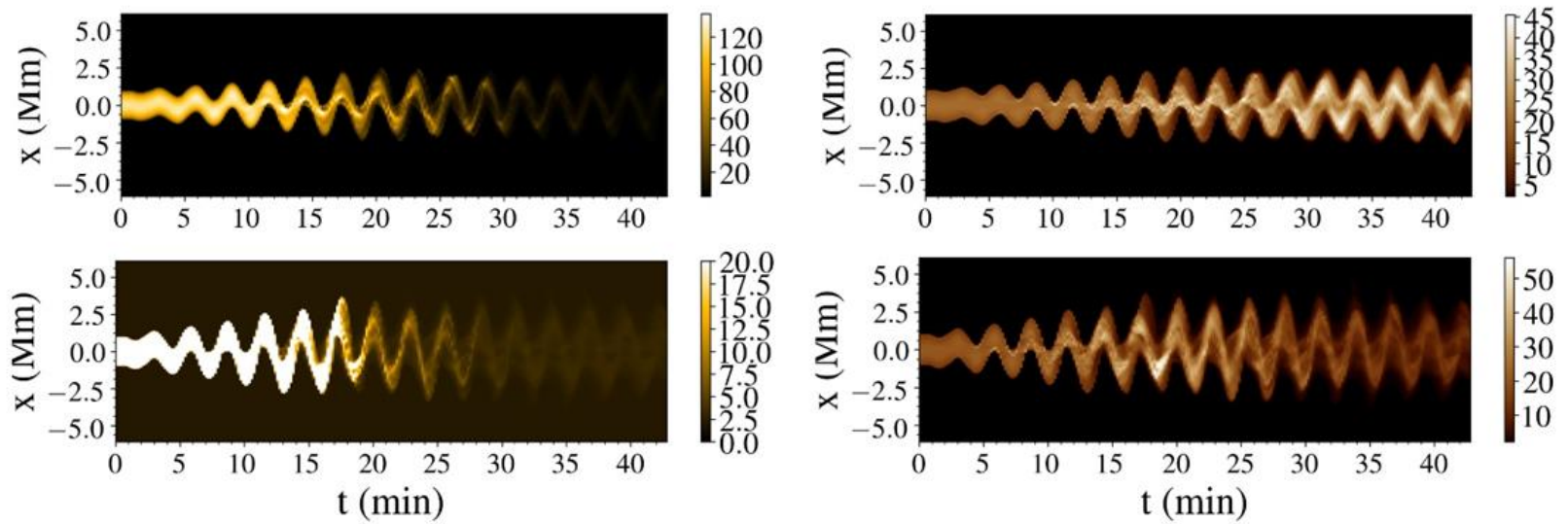


**Figure a:** Time distance maps of the integrated emission for models **D2 (top)** and **D4 (bottom)**. The synthetic data the SDO/AIA 171 (**left**) and 193 (**right**) channels, at a  $0^\circ$  angle from the POS.

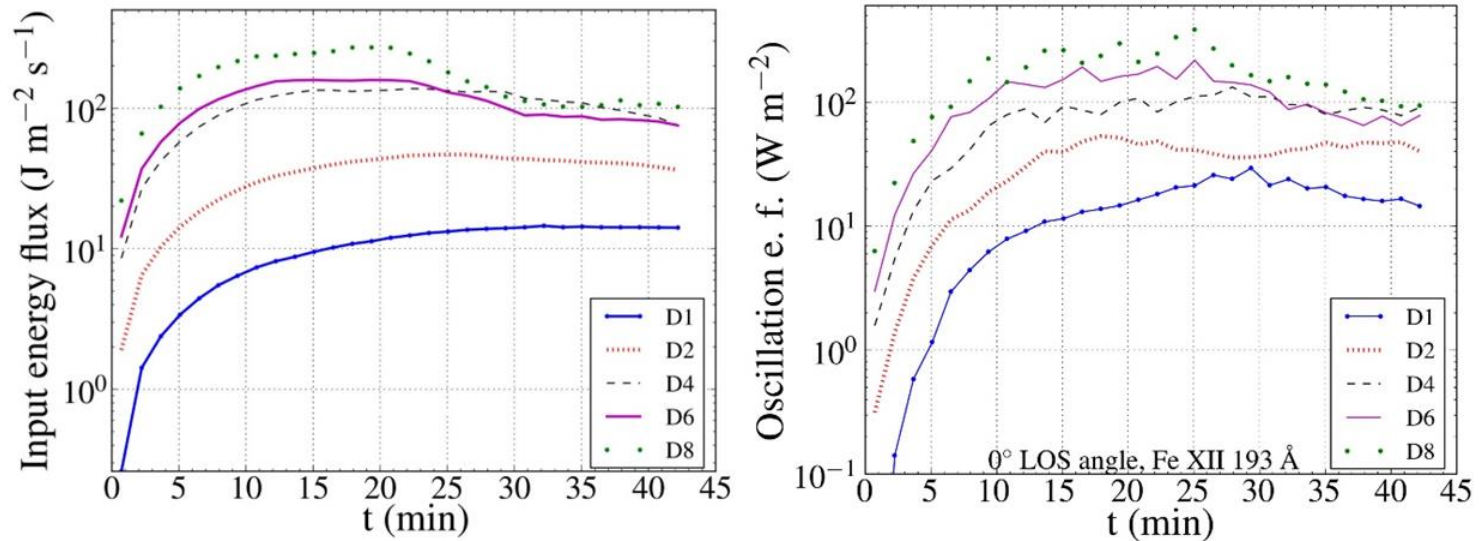


**Figure b:** Left panel: average input energy flux from each driver. Right panel: the sum of energy fluxes estimated from the Doppler velocities, from the non-thermal line width and from tracking the oscillations.

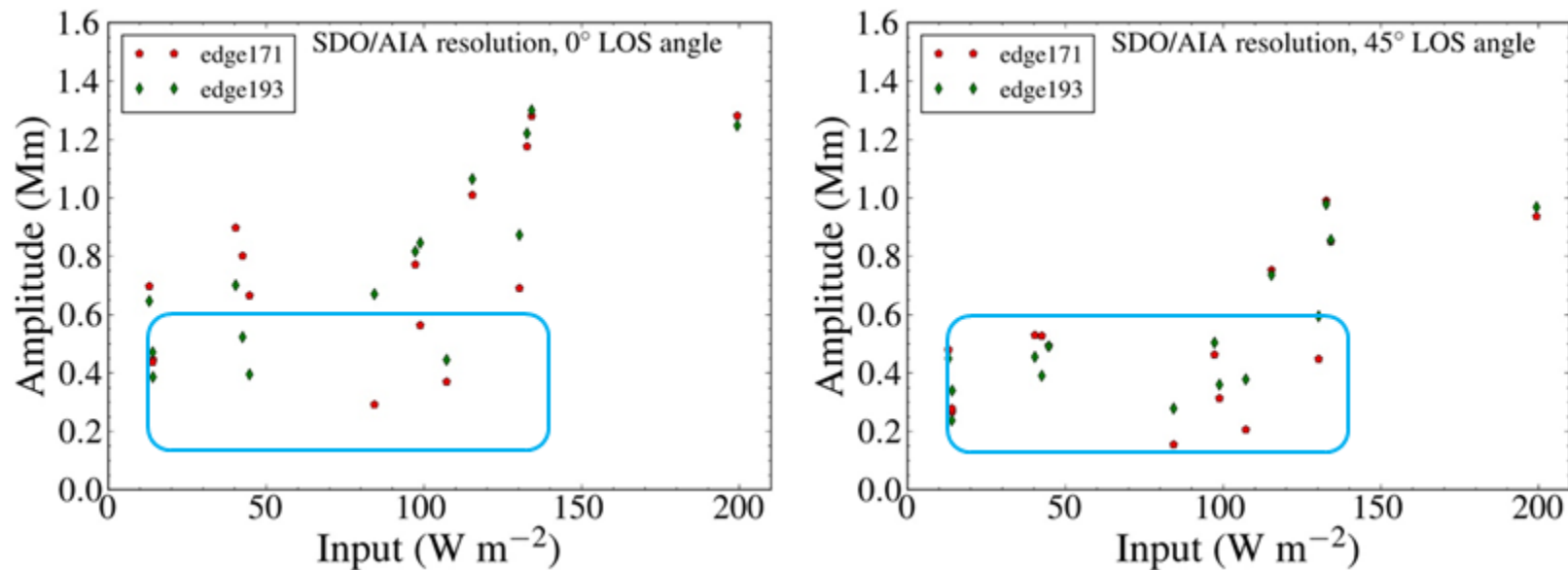


**Figure:** Average oscillation amplitudes as a function of the average energy input for each model. Data from the AIA 193 and 171 channels, at a 0° and 45° LOS angle.

## Emission maps from simulations of decayless oscillations

1. The strong out-of-phase flows from the KHI, and the effects of mixing on the emission lead to saturation of the observed oscillation amplitude.
2. The obtained amplitudes reach the upper limit of decayless oscillations.
3. Weaker drivers can produce larger apparent amplitudes.
4. Small-amplitude oscillations can potentially sustain the Quiet Sun.
5. Solving this uncertainty requires (a) spectroscopic data and (b) better understanding of the driving mechanism.
6. Most of the considered driving mechanisms should be located in the lower atmosphere!

## Summary

- Development of the KH instability.
- The spatially extended TWIKH rolls deform the initially monolithic cross-section.
- TWIKH rolls spread phase mixing over a larger area. More efficient energy dissipation.
- Synthetic data show oscillation amplitudes within the range of decayless oscillations.
- Small-amplitude oscillations can potentially provide enough energy flux to sustain the Quiet Sun.

## Open questions

- Our setup simulates only the coronal part of coronal loops. No chromosphere or TR considered.
- High values of dissipation can suppress the development of the instability. Observational proof of this instability in flux tubes (e.g. loops, spicules etc) is needed.
- The mechanism producing the decayless oscillations is still under debate.
- They are treated as (a) a self-oscillatory process from continuous flows across loops (Nakariakov et al. 2016) , (b) LOS effects from the KHI (Antolin et al. 2016), (c) driven waves (Karampelas et al. 2019a,b; Guo et al. 2018;...), or mode conversion from p modes (Riedl et al. 2019).
- Observational data from chromospheric plasma and the lower solar atmosphere is needed for answering this question.